

# Long-term imatinib therapy promotes bone formation in CML patients

Stephen Fitter,<sup>1</sup> Andrea L. Dewar,<sup>1</sup> Panagiota Kostakis,<sup>1</sup> L. Bik To,<sup>2</sup> Timothy P. Hughes,<sup>2</sup> Marion M. Roberts,<sup>2</sup> Kevin Lynch,<sup>3</sup> Barrie Vernon-Roberts,<sup>4</sup> and Andrew C. W. Zannettino<sup>1</sup>

<sup>1</sup>Bone and Cancer Research Laboratories, and <sup>2</sup>Division of Haematology, Institute of Medical and Veterinary Science (IMVS), The Hanson Institute, Adelaide; <sup>3</sup>Medical Oncology, Novartis Pharmaceuticals, Sydney; and <sup>4</sup>Adelaide Centre for Spinal Research, IMVS, The Hanson Institute, Adelaide, Australia

**Imatinib inhibits tyrosine kinases important in osteoclast (c-Fms) and osteoblast (platelet-derived growth factor receptor [PDGF-R], c-Abl) function, suggesting that long-term therapy may alter bone homeostasis. To investigate this question, we measured the trabecular bone volume (TBV) in iliac crest bone biopsies taken from chronic myeloid leukemia (CML) patients at diagnosis and again after 2 to 4 years of imatinib therapy. Half the patients (8 of 17) showed a substantive increase in TBV (> 2-fold), after imatinib therapy, with the TBV in the posttreat-**

**ment biopsy typically surpassing the normal upper limit for the patient's age group. Imatinib-treated patients exhibited reduced serum calcium and phosphate levels with hypophosphatemia evident in 53% (9 of 17) of patients. In vitro, imatinib suppressed osteoblast proliferation and stimulated osteogenic gene expression and mineralized-matrix production by inhibiting PDGF receptor function. In PDGF-stimulated cultures, imatinib dose-dependently inhibited activation of Akt and Crk-L. Using pharmacologic inhibitors, inhibition of PI3-kinase/Akt activa-**

**tion promoted mineral formation, suggesting a possible molecular mechanism for the imatinib-mediated increase in TBV in vivo. Further investigation is required to determine whether the increase in TBV associated with imatinib therapy may represent a novel therapeutic avenue for the treatment of diseases that are characterized by generalized bone loss. (Blood. 2008;111:2538-2547)**

© 2008 by The American Society of Hematology

## Introduction

Imatinib mesylate (imatinib, Gleevec, or STI-571; Novartis, Basel, Switzerland) is highly effective in treating chronic myeloid leukemia (CML) by targeting the constitutively active tyrosine-kinase domain of *BCR-ABL* and successfully competing for adenosine triphosphate (ATP) binding. Imatinib also binds to other receptor (c-Kit, platelet-derived growth factor [PDGF-R], c-Fms) and nonreceptor (Arg, Lck) tyrosine kinases, thereby extending the therapeutic range of imatinib to include treatment of gastrointestinal stromal tumors (GIST),<sup>1</sup> myeloproliferative disorders,<sup>2</sup> and other malignant diseases characterized by oncogenic rearrangements of these target genes.

We have demonstrated that imatinib binds to the kinase domain of c-Fms, the receptor for macrophage colony-stimulating factor (M-CSF).<sup>3</sup> M-CSF induces differentiation of peripheral blood precursor cells into functional, bone-resorbing osteoclasts.<sup>4</sup> In vitro, imatinib inhibits both osteoclast differentiation and function by blocking M-CSF activity. Furthermore, oral administration of imatinib in mice decreases lacunae formation consistent with a reduction in osteoclast activity.<sup>5</sup>

The balance between bone resorption by osteoclasts and bone formation by osteoblasts is essential for maintaining bone homeostasis. Osteoblasts are specialized cells responsible for the synthesis of bone matrix after the removal of unwanted or effete bone by osteoclasts. Osteoblasts are derived from precursor mesenchymal stem cells that reside within the bone marrow. These stem cells display the capacity to differentiate into osteoblasts, chondrocytes,

adipocytes, or myocytes.<sup>6-8</sup> The proliferation, differentiation, and maturation of osteoblasts is controlled by a number of signaling pathways that include imatinib-sensitive tyrosine kinases PDGF-R and c-Abl. In vitro, PDGF promotes osteoblast proliferation while acting to suppress differentiation.<sup>9-11</sup> In vivo, localized administration of PDGF accelerates fracture healing,<sup>12</sup> and systemic administration increases bone density in ovariectomized rats.<sup>13</sup> In mice devoid of c-Abl, osteoblasts fail to mature, leading to an osteoporotic phenotype.<sup>14</sup>

In light of the inhibitory action of imatinib on c-Fms, PDGF-R, and c-Abl, extended exposure of CML and GIST patients to imatinib may perturb the balance between bone resorption and synthesis. In support of this hypothesis, 2 recent studies demonstrated that CML and GIST patients undergoing imatinib therapy had indicators of altered bone metabolism in their peripheral blood.<sup>15,16</sup> Moreover, these studies showed that changes in bone metabolism, as measured by serum markers of bone turnover, occurred within 3 months of commencing imatinib therapy.

In this current study, we sought to determine the effects of long-term imatinib therapy on bone remodeling by performing a retrospective histomorphometric analysis of iliac crest trephines taken from CML patients before and after 2 to 4 years of imatinib treatment. Furthermore, using human primary osteoblast culture systems, we examined the effect of imatinib on osteoblast function to provide mechanistic insights into the effects of imatinib on skeletal metabolism.

Submitted July 30, 2007; accepted November 24, 2007. Prepublished online as *Blood* First Edition paper, November 27, 2007; DOI 10.1182/blood-2007-07-104281.

An Inside *Blood* analysis of this article appears at the front of this issue.

The online version of this article contains a data supplement.

The publication costs of this article were defrayed in part by page charge payment. Therefore, and solely to indicate this fact, this article is hereby marked "advertisement" in accordance with 18 USC section 1734.

© 2008 by The American Society of Hematology

## Methods

### Patients

A retrospective study of 29 white CML patients was conducted in accordance with procedures approved by the Royal Adelaide Hospital Ethics Committee. Informed consent was obtained in accordance with the Declaration of Helsinki. Of the 29 patients, 17 patients (5 women, 12 men; median age at diagnosis, 53 years; range, 32-70 years) received imatinib mesylate therapy (400 mg/day) for 17 to 62 (median, 25) months. The remaining 12 patients (4 women, 8 men; median age at diagnosis, 51 years; range, 27-67 years) received  $\alpha$ -interferon therapy ( $3 \times 10^6$  to  $9 \times 10^6$  units/day) for 12 to 108 (median, 20.5) months. For each patient, peripheral blood counts and bone marrow cellularity were assessed at diagnosis and again after either imatinib or  $\alpha$ -interferon therapy, to determine disease status; these data can be found in Table S1 (available on the *Blood* website; see the Supplemental Materials link at the top of the online article).

### Bone histomorphometry

Histomorphometric assessments were performed on posterior superior iliac spine trephine biopsies (2 mm diameter; median length, 15 mm; range, 10-27 mm) obtained at diagnosis and again after imatinib or  $\alpha$ -interferon therapy. Briefly, biopsies were fixed in mercuric chloride fixative (0.22 M mercury (II) chloride, 10% formaldehyde, 1.5% acetic acid) for 2 hours at room temperature and rapidly decalcified in 9.5% nitric acid/1% EDTA (ethylenediaminetetraacetic acid) solution, then neutralized in 6% aqueous  $\text{Na}_2\text{SO}_4$  before being processed into paraffin wax. Sections measuring 5  $\mu\text{m}$  were routinely stained with hematoxylin-eosin and, selectively, with Gomori reticulin, then were blind-coded before assessment by a pathologist who has extensive experience with bone morphometry (B.V.-R.). Trabecular bone volume (TBV; the percentage of the volume of the biopsy [bone and soft tissue] that is composed of trabecular bone) and hematopoietic tissue volume (the percentage of soft tissue that is composed of hematopoietic tissue) were determined by analyzing the entire length of 2 longitudinal sections, cut at different planes in the same bone core using point counting with an ocular-mounted Weibel II graticule, at 40 $\times$  magnification, as previously described.<sup>17</sup> Because variances among TBV measurements were typically less than 1%, singular TBV values are presented. The normal iliac crest TBV ranges referred to in this study are those previously determined after examination of samples from 135 white subjects (105 from subjects after unexpected deaths, and 30 from living volunteers) as measured using point counting.<sup>18</sup>

### Blood assessment

Routine serum biochemistry was performed when bone biopsies were obtained in the Division of Clinical Pathology, Diagnostic Services Laboratory, Institute of Medical and Veterinary Sciences, Adelaide, South Australia, using an Olympus AU5400 Chemistry-Immuno analyser (Olympus Europe, Hamburg, Germany) according to institutional protocols. Levels of serum phosphate, sodium, potassium, total serum calcium, ionized calcium, and serum alkaline phosphatase were obtained from archived records.

### Mesenchymal cell isolation

Mesenchymal cells were grown from bone chips recovered from posterior iliac crest bone marrow aspirates. Aspirates were obtained from healthy adult volunteers, after informed consent in accordance with procedures approved by the Royal Adelaide Hospital Ethics Committee. Cells were cultured in  $\alpha$ -minimal essential medium ( $\alpha$ -MEM; JRH Biosciences, Lenexa, KS), supplemented with 10% fetal calf serum (FCS), 2 mM L-glutamine, 100  $\mu\text{M}$  L-ascorbate-2-phosphate, 50 IU/mL penicillin, 50  $\mu\text{g}/\text{mL}$  streptomycin sulfate, 1 mM sodium pyruvate (SAFC Biosciences, Brooklyn, Australia), and 15 mM HEPES (N-2-hydroxyethylpiperazine-N'-2-ethanesulfonic acid) buffer. Single-cell

suspensions were obtained from confluent primary cultures by enzymatic digestion with collagenase (1 mg/mL; Collagenase type I; Worthington Biochemical, Freehold, NJ) and dispase (1 mg/mL; Neutral Protease grade 2; Roche Diagnostics, Mannheim, Germany). To stimulate osteogenesis, cells were cultured with reduced FCS (2% [vol/vol]) and media supplemented with dexamethasone sodium phosphate ( $10^{-7}$  M; Mayne Pharma, Mulgrave, Australia) and 1.8 mM  $\text{KH}_2\text{PO}_4$ .<sup>19</sup>

### Cell-cycle analysis

Mesenchymal cells were seeded at  $10^5$  cells per flask in 25-cm<sup>2</sup> tissue-culture flasks and treated with and without 3.0  $\mu\text{M}$  imatinib for 7 days. Cells were harvested, enumerated and washed twice with phosphate-buffered saline (PBS) before fixation in ice-cold 70% (vol/vol) ethanol for 2 hours at 4°C. Fixed cells were washed once in PBS, then incubated in propidium iodide/Triton X-100 staining solution (0.2 mg/mL DNase-free RNase A (Sigma-Aldrich, St Louis, MO), 20  $\mu\text{g}/\text{mL}$  propidium iodide (PI; Aldrich Chemical, Milwaukee, WI) and 0.1% (vol/vol) Triton X-100 (MP Biomedicals, Solon, OH) in PBS for 15 minutes at 37°C. The distribution of cells was determined by analysis on a Cytomics FC500 flow cytometer (Beckman Coulter, Fullerton, CA).

### Cell-proliferation assay

Mesenchymal cells were resuspended in 0.1% bovine serum albumin (BSA) in HEPES-buffered saline and stained with 10  $\mu\text{M}$  carboxyfluorescein diacetate succinimidyl ester (CFSE; Invitrogen, Carlsbad, CA) for 10 minutes at 37°C. Cells were washed twice in culture media, seeded at  $10^5$  cells per flask in 25-cm<sup>2</sup> tissue-culture flasks, and treated with and without 3.0  $\mu\text{M}$  imatinib for 7 days. Control flasks were either unstained or treated with colcemid (100 ng/mL; Invitrogen). Cells were analyzed for CFSE fluorescence using a Cytomics FC500 flow cytometer. Data were analyzed using ModFit LT for Win 32 Software (version 3.0; Verity Software House, Topsham, ME), to determine the number of cell divisions (based on undivided colcemid-treated cultures), as well as the percentage of cells in each division.

### Mineralization assay

Mesenchymal cells were seeded into 96-well plates ( $8 \times 10^3$  cells/well) in media supplemented with  $\text{KH}_2\text{PO}_4$  (1.8 mM). To assess the effects of PDGF on mineralization, cultures were supplemented with 10 ng/mL rhPDGF-BB (Peprotech, Rocky Hill, NJ). Inhibitors AG-1295 (25  $\mu\text{M}$ ) and LY294002 (5  $\mu\text{M}$ ; both from Sigma-Aldrich) were added to assess the effects of blocking PDGF-R and PI3 kinase, respectively. Dimethyl sulfoxide (DMSO; 0.1%) was included in control cultures. Medium was changed twice weekly, and mineralized matrix was quantified by measuring  $\text{Ca}^{2+}$  levels (Cresolphthalein method; Thermo Electron, Ulm, Germany) after 4 weeks. Calcium levels were normalized to the number of cells per well. To identify lipid-laden fat cells, formalin-fixed cells were stained with Oil Red O (ICN Biomedicals, Aurora, OH) as described.<sup>20</sup> Data are representative of results from 3 donors.

### Quantitative real-time PCR

Mesenchymal cells were seeded into 24-well plates ( $5 \times 10^4$  cells/well) in osteogenic media supplemented with 3.0  $\mu\text{M}$  imatinib and total RNA was isolated at weekly intervals using Trizol (Invitrogen). cDNA was prepared from 1  $\mu\text{g}$  total RNA using Superscript III and random hexamers in accordance with manufacturer instructions (Invitrogen). Primer pairs were as follows: bone morphogenic protein-2 (*BMP-2*) forward, 5'-tcaagccaacaacaacagc-3'; reverse, 5'-acgtctcaatggcatga-3'; osterix (*OSX*) forward, 5'-ctcgaggactcaacaactct-3'; reverse, 5'-gagccatagggtgtgtc-3'; adipocyte lipid binding protein (*ALBP*) forward, 5'-agtcaagagcaccataacccttaga-3'; reverse, 5'-ccttgcttatgctctctcataa-3'; peroxisome proliferator-activated receptor gamma (*PPAR $\gamma$ 2*) forward, 5'-tcaagagtgaggcagtgctc-3'; reverse, 5'-tcaagagtgaggcagtgctc-3'; CCAAT/enhancer-binding protein- $\alpha$  (*C/EBP $\alpha$* ) forward, 5'-gggcaaggccaagaagtc-3'; reverse, 5'-ttgtcactgtcagctcag-3';  $\beta$ -actin forward, 5'-gatcattgctctctcagc-3'; reverse, 5'-gtcatagctccctagaagcat-3'. Polymerase chain reactions (PCRs) were performed in a

Rotor-Gene 6000 real-time rotary analyzer (Corbett Research, Mortlake, Australia), and the fold-changes in expression were calculated relative to  $\beta$ -actin.

### Western blotting

For pulse experiments, mesenchymal cells were grown to 80% to 90% confluence in 10-cm dishes and were serum deprived for 12 hours before stimulation. Cells were exposed to drugs (at indicated concentrations) for 1 hour, then stimulated with serum-free media supplemented with 10 ng/mL PDGF-BB for the indicated times. For long-term osteogenic cultures, cells were cultured for 14 days under osteoinductive conditions in the presence or absence of 3  $\mu$ M imatinib. Cell lysates were obtained as previously described<sup>21</sup> and equivalent amounts (50  $\mu$ g) of protein were separated on 10% sodium dodecyl sulfate-polyacrylamide gel electrophoresis (SDS-PAGE) gels and transferred to polyvinylidene difluoride membrane (PVDF) membranes. Membranes were probed with phosphorylation-specific antibodies to phospho-Erk1/2 (Thr202/Tyr204; Cell Signaling Technology, Danvers, MA), phospho-p38 (Thr180/Tyr182), phospho-Akt (Ser473), phospho-Crk-L (Tyr207) and  $\alpha$ -tubulin (Abcam, Cambridge, MA). Bound antibody was detected using an alkaline-phosphatase-conjugated secondary antibody then visualized using a Typhoon 9410 imager (GE Healthcare, Little Chalfont, United Kingdom) in the presence of an enhanced chemifluorescence substrate. Quantitative analysis was performed using ImageQuant imaging software (version 5.2; GE Healthcare). Data are representative of results from cell cultures derived from 3 different donors.

### Statistical analysis

Statistical analysis was performed using SigmaStat (version 3.0; SPSS, Chicago, Illinois). The *t* test was used for comparison of paired data and the Spearman rank correlation test was used for the correlation analysis. Two-sided *P* values less than .05 were considered statistically significant.

## Results

### CML patients have increased trabecular bone in the iliac crest after long-term imatinib therapy

Imatinib mesylate inhibits tyrosine kinases important in osteoclast (c-Fms) and osteoblast (PDGF-R, c-Abl) function, suggesting that long-term exposure to imatinib may alter bone homeostasis. To investigate this possibility, we performed a retrospective histomorphometric analysis of posterior iliac crest bone trephines taken at diagnosis of CML and compared these to trephines taken from the same patients after imatinib therapy.

Analysis of bone trephines taken at diagnosis showed that TBV was within the age-matched normal range<sup>18</sup> in 11 patients, below normal in 4 patients, and exceeded the normal range in 2 patients (Table 1). After imatinib therapy, a significant increase in TBV ( $P = .005$ , paired *t* test) was observed, with 8 patients (> 50%) showing at least a 2-fold increase (range, 1.2-fold to 12.8-fold; mean  $\pm$  SD,  $2.9 \pm 2.8$ ; Table 1 and Figure 1). The increase in TBV occurred regardless of the sex and age of the patient, duration of treatment, or bone volume before treatment. A significant degree of osteoporosis, observed in 4 patients at initial diagnosis, did not prevent a marked increase in their bone volumes after imatinib therapy (1.9-fold for 1 patient, 3.7-fold for 2 patients, and 12.8-fold for 1 patient; Table 1), whereas the patient who had an excess of bone in the initial biopsy was the sole patient whose second biopsy showed a marked (50%) reduction in bone volume (Table 1). Microscopy of the intertrabecular marrow tissues at diagnosis showed hypercellular myelopoiesis surrounding trabecular bone (Figure 1B,D). After imatinib therapy, the increase in trabecular

bone was clearly evident, as were adipocytes, which form part of the reconstituted marrow tissue (Figure 1C,E).

Proliferation of leukemia cells in the bone marrow results in a hypercellular environment dominated by myeloid cells, which occurs without gross changes in bone morphometry.<sup>22,23</sup> Because imatinib restored the bone marrow to normocellularity or near normocellularity (Table S1), the increase in TBV after imatinib therapy may be an indirect mechanism associated with reconstitution of bone marrow cells. To investigate this question, we compared the TBV of bone biopsies taken at diagnosis of CML to biopsies taken after  $\alpha$ -interferon therapy (median, 20.5 months; range, 12-108 months; Table 1). Of the 12  $\alpha$ -interferon patients examined, 8 patients achieved a complete hematologic response (CHR)<sup>24</sup> and normocellular marrow, and the remaining patients achieved only a partial hematologic response (Table S1). In contrast to the imatinib cohort, no significant difference in TBV before and after  $\alpha$ -interferon treatment was observed in the 8 patients who achieved CHR ( $P = .36$ , paired *t* test; Table 1). Analysis of all  $\alpha$ -interferon-treated patients, irrespective of their response to therapy, also failed to reveal a significant difference in TBV before and after therapy ( $P = .35$ , paired *t* test, Table 1).

### CML patients have reduced serum phosphate and calcium levels after long-term imatinib therapy

Previous studies have demonstrated that serum phosphate and calcium levels are reduced in some CML and GIST patients receiving imatinib therapy,<sup>15,16</sup> with changes in phosphate levels occurring within the first 3 months of treatment. To investigate whether serum phosphate and calcium levels were reduced in long-term imatinib recipients, we compared serum biochemistry data obtained at the time of diagnosis to that obtained at the time of the second postimatinib biopsy (paired imatinib group,  $n = 17$ ). After imatinib therapy, there was a significant decrease in total serum phosphate (mean  $\pm$  SD,  $1.04 \pm 0.18$  mM, compared with  $0.8 \pm 0.13$  mM,  $P < .001$ , paired *t* test) with hypophosphatemia (serum phosphate level < 0.8 mM) evident in 9 patients (Table S2). Significant differences in total serum calcium ( $2.32 \pm 0.11$  mM, compared with  $2.2 \pm 0.12$  mM,  $P < .001$ ) and ionized calcium ( $1.18 \pm 0.05$  mM, compared with  $1.14 \pm 0.05$  mM,  $P = .002$ ) were also observed in samples taken before and after imatinib therapy (Table 2). No significant difference was observed for serum alkaline phosphatase activity or serum  $\text{Na}^+$  or  $\text{K}^+$  levels (data not shown).

We next examined whether the reduction in serum phosphate and calcium levels observed after imatinib therapy was related to CML disease regression by comparing serum biochemistry in patients before and after  $\alpha$ -interferon therapy. No statistical differences in serum phosphate or in total or ionized calcium levels were observed after  $\alpha$ -interferon treatment (Table 2).

### Increased TBV correlates with decreased serum phosphate and calcium in imatinib patients

We performed a correlation analysis to determine the relationship between TBV and serum electrolyte levels. A negative correlation was observed both between TBV and serum phosphate levels ( $r = -0.48$ ,  $P = .004$ , Table 3) and between TBV and total serum calcium levels ( $r = -0.42$ ,  $P = .014$ , Table 3), suggesting that increased TBV is associated with decreased serum phosphate and total calcium. A positive correlation was observed between serum phosphate levels and total calcium levels ( $r = 0.467$ ,  $P = .006$ , Table 3), as well as between serum phosphate levels and ionized calcium levels ( $r = 0.48$ ,  $P = .004$ , Table 3), suggesting that

Table 1. Trabecular bone volume as measured at diagnosis of CML and following imatinib mesylate or  $\alpha$ -interferon therapy

| Patient details   |     |       | Trabecular bone volume (TBV)* |        |                 |       | Fold change |
|---|-----|-------|-------------------------------|--------|-----------------|-------|-------------|
|   |     |       | At diagnosis                  |        | After treatment |       |             |
| Age   | Sex | Time† | TBV                           | Range‡ | TBV             | Range |             |
| <b>Imatinib treated patients (n = 17)</b>                       |     |       |                               |        |                 |       |             |
| 32  | F   | 22    | 8                             | BN     | 30              | AN    | 3.7         |
| 37  | F   | 17    | 25                            | N      | 26              | N     | no change   |
| 38  | M   | 48    | 17                            | N      | 24              | N     | 1.4         |
| 39  | M   | 23    | 27                            | N      | 53              | AN    | 2.0         |
| 41  | M   | 18    | 22                            | N      | 36              | AN    | 1.6         |
| 42  | M   | 4     | 28                            | BN     | 30              | AN    | 3.7         |
| 46  | M   | 23    | 33                            | AN     | 18              | N     | -0.5        |
| 53  | M   | 33    | 16                            | N      | 50              | AN    | 3.1         |
| 63  | M   | 2     | 57                            | BN     | 90              | AN    | 12.8        |
| 63  | M   | 53    | 11                            | N      | 12              | N     | no change   |
| 65  | M   | 35    | 11                            | N      | 27              | AN    | 2.7         |
| 69  | M   | 54    | 10                            | BN     | 19              | N     | 1.9         |
| 70  | M   | 19    | 14                            | N      | 42              | AN    | 3.0         |
| 70  | M   | 25    | 16                            | N      | 26              | AN    | 1.6         |
| 52  | F   | 23    | 24                            | AN     | 29              | AN    | 1.2         |
| 54  | F   | 62    | 18                            | N      | 37              | AN    | 2.0         |
| 66  | F   | 23    | 14                            | N      | 25              | AN    | 1.8         |
| P value§  |     |       |                               |        | P = .005        |       |             |
| <b><math>\alpha</math>-interferon treated patients (n = 12)</b> |     |       |                               |        |                 |       |             |
| 27  | M   | 12    | 16                            | BN     | 23              | N     | 1.4         |
| 31  | F   | 18    | 11                            | BN     | 10              | BN    | no change   |
| 36  | F   | 18    | 22                            | BN     | 19              | BN    | no change   |
| 45  | M   | 45    | 14                            | BN     | 28              | AN    | 2.0         |
| 47  | M   | 12    | 11                            | BN     | 22              | N     | 2.0         |
| 48  | M   | 18    | 13                            | BN     | 26              | N     | 2.0         |
| 55  | M   | 45    | 15                            | N      | 21              | AN    | 1.4         |
| 55  | M   | 23    | 20                            | N      | 20              | N     | no change   |
| 65  | M   | 31    | 28                            | N      | 16              | N     | -0.6        |
| 67  | M   | 18    | 26                            | AN     | 32              | N     | 1.2         |
| 54  | F   | 18    | 34                            | AN     | 24              | AN    | -0.7        |
| 57  | F   | 36    | 17                            | N      | 15              | N     | no change   |
| P value   |     |       |                               |        | P = .35         |       |             |
| P value¶  |     |       |                               |        | P = .36         |       |             |

N indicates normal; AN, above normal; and BN, below normal.

\*Percent of the volume of the biopsy (bone and soft tissue) composed of trabecular bone.

†Months of therapy at the time of the second bone biopsy.

‡Normal TBV ranges: adults younger than 50 years, 18% to 26%; men 50 years and older, 12% to 21%; women 50 years and older, 11% to 17%.<sup>18</sup>

§P value describe the comparison of paired TBV data (before and after imatinib) using paired *t* test.

||P value describe the comparison of paired TBV data (before and after  $\alpha$ -interferon), for patients who achieved CHR and normocellular marrow after treatment ( $n=8$ ), using paired *t* test.

¶P value describe the comparison of paired TBV data (before and after  $\alpha$ -interferon,  $n=12$ ) using paired *t* test.

changes in serum phosphate are associated with a concomitant change in serum calcium.

### Imatinib inhibits mesenchymal cell proliferation

The increase in TBV after imatinib therapy suggests that imatinib modulates bone remodeling. Although we previously demonstrated that imatinib suppresses bone resorption through inhibition of osteoclast function,<sup>3,5</sup> little is known of the effect of imatinib on bone-forming cells and their mesenchymal precursors. To investigate this, we used bone explant cultures derived from posterior superior iliac spine bone trephines from healthy donors. These cultures contain a mixture of mesenchymal cells that can differentiate into osteoblasts, adipocytes, and chondrocytes under appropriate growth conditions.<sup>20</sup> Initially, we examined the effect of therapeutic concentrations of imatinib<sup>25</sup> on cell proliferation using CFSE, a fluorescent dye that is distributed equally between daughter cells after cell division<sup>26</sup> (Figure 2A). In the absence

of imatinib, cells underwent a maximum of 5 divisions, with the highest percentage of cells (48.4%) undergoing 4 divisions (Figure 2A). In contrast, cells cultured with 3.0  $\mu$ M imatinib underwent a maximum of 4 divisions, with the highest percentage of cells undergoing 3 divisions (43.96%; Figure 2A). As well as decreasing the overall rate of cell division, imatinib also inhibited proliferation of the initial starting population of cells. Specifically, the percentage of cells which did not undergo any cell division ( $D_0$ ) was higher in cultures treated with imatinib (5.22%) than in untreated cultures (2.43%; Figure 2A). To determine whether imatinib induced apoptosis, the effect of imatinib on cell cycling was examined using propidium iodide (PI; Figure 2B). Approximately 83% of cells accumulated in the  $G_1$  phase of the cell cycle, both in the presence and in the absence of imatinib (3  $\mu$ M), and no difference in the percentage of cells in the sub- $G_1/G_0$  (apoptotic), S, or  $G_2$  phases was observed in cultures treated with imatinib, compared with controls.

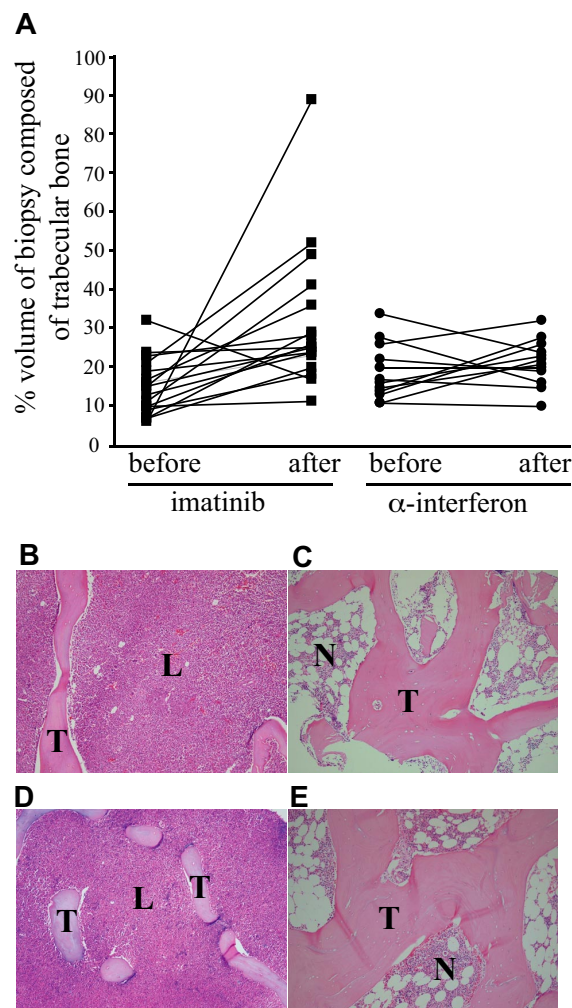


**Figure 1. CML patients treated with imatinib have increased iliac crest TBV and altered bone marrow cellularity.** Sections of posterior superior iliac spine bone trephines taken at diagnosis were analyzed by histomorphometry and compared with trephines obtained from the same patients after imatinib or  $\alpha$ -interferon therapy. (A) Changes in TBV before and after imatinib (■) or  $\alpha$ -interferon (●) therapy are shown as lines for individual patients. Bone marrow cellularity of patients at diagnosis of CML (patient 1 [panel B] and patient 2 [panel D]) and after 42 months (patient 1 [panel C]) and 33 months (patient 2 [panel E]) of imatinib therapy is shown. T indicates trabecular bone; N, normal marrow; and L, leukemic cells. Original magnification 40 $\times$  for panels B-E. Micrographs were acquired with a CKX41 inverted microscope (Olympus, Center Valley, PA) and images captured using DPIX image capture system (Olympus).

#### Imatinib promotes mineralized-matrix production in vitro

To examine the effect of imatinib on osteoblast function, we cultured cells under osteoinductive conditions in the presence of various concentrations of imatinib. Under osteoinductive condi-

tions, osteoblast cells isolated from bone trephine explant cultures form a mineralized extracellular matrix in the presence of inorganic phosphate.<sup>19,27</sup> Addition of imatinib resulted in a dose-dependent increase in mineral formation, with a 2.5-fold increase in the concentration of acid-solubilized calcium at 3  $\mu$ M imatinib compared with controls (Figure 3A). Energy dispersive X-ray analysis of this mineral revealed calcium to phosphorous ratios consistent with hydroxyapatite (data not shown).

We next examined whether the imatinib-induced increase in mineralization was due to an inhibition of the platelet-derived growth factor (PDGF) receptor. PDGF is a potent mitogen for osteoblasts and is locally synthesized by skeletal cells. While it increases the proliferation of cells of the osteoblast lineage, PDGF significantly inhibits bone matrix formation.<sup>9-11</sup> Addition of PDGF to cultures significantly reduced mineral formation, and this effect was overcome by the addition of 3  $\mu$ M imatinib (Figure 3B). Surprisingly, under osteogenic conditions, lipid droplets were observed in a subpopulation of cells, suggesting that in addition to inducing osteogenic differentiation, imatinib induced adipogenesis (Figure 3C).

#### Imatinib modulates the expression of osteoblastogenic and adipogenic genes

To further investigate the effect of imatinib on mesenchymal cell differentiation, we analyzed the effect of 3  $\mu$ M imatinib on the expression of osteoblastogenic and adipogenic genes on days 1, 7, and 14 of culture. Addition of imatinib significantly increased expression of the osteoblastogenic genes *BMP-2* and *OSX* 2.6-fold and 3.9-fold, respectively, on day 14 (Figure 4A). Imatinib did not affect the expression of other osteoblast-associated genes, including *Cbfa-1* (*Runx2*) and *Wnt-10b*, at the time points examined (data not shown). Consistent with the appearance of adipocytes in imatinib-treated cultures, imatinib significantly increased the expression of *ALBP* (171-fold), *PPAR $\gamma$ 2* (14-fold), and *C/EBP $\alpha$*  (3-fold) on day 14 of culture.

#### Imatinib is a potent inhibitor of PDGF-induced Akt and Crk-L activation

We next examined the effect of imatinib on PDGF signaling pathways in bone explant cultures. Stimulation of cultures with PDGF rapidly activated Erk1/2, p38 MAPK, Akt (a primary PI3-kinase substrate) and Crk-L, an adaptor protein that is activated by c-Abl<sup>28</sup> (Figure 5A). JNK (SAPK) was not activated by PDGF in these cells (data not shown). Addition of imatinib (3  $\mu$ M) resulted in a modest reduction in p38 activation, but significantly reduced activation of Akt and completely inhibited Crk-L activation. In contrast, imatinib had no effect on PDGF-induced Erk1/2 activation. The inhibition of PDGF-induced p38, Akt, and Crk-L activation by imatinib was dose dependent, with activation levels reduced to unstimulated levels at concentrations exceeding 1  $\mu$ M

**Table 2. Serum electrolyte levels as measured at diagnosis of CML and after imatinib mesylate or  $\alpha$ -interferon therapy**

| Variable                      | Treatment         |                 |        |                               |                 |     |     |      |
|-------------------------------|-------------------|-----------------|--------|-------------------------------|-----------------|-----|-----|------|
|                               | Imatinib (n = 17) |                 |        | $\alpha$ -interferon (n = 12) |                 |     |     |      |
|                               | Before            | After           | P*     | Before                        | After           | P*  | P†  | P‡   |
| Phosphate, mM                 | 1.04 $\pm$ 0.18   | 0.8 $\pm$ 0.13  | < .001 | 1.09 $\pm$ 1.03               | 1.03 $\pm$ 0.15 | .37 | .44 | .001 |
| Total Ca <sup>2+</sup> , mM   | 2.32 $\pm$ 0.11   | 2.20 $\pm$ 0.13 | < .001 | 2.30 $\pm$ 0.1                | 2.26 $\pm$ 0.1  | .20 | .59 | .23  |
| Ionized Ca <sup>2+</sup> , mM | 1.18 $\pm$ 0.05   | 1.14 $\pm$ 0.05 | < .005 | 1.17 $\pm$ 0.04               | 1.14 $\pm$ 0.05 | .16 | .46 | .06  |

Values shown are means plus or minus standard deviations.

\*P values for the comparison of paired data (before and after) using paired t test.

†P values describe the comparison of before-imatinib treatment data with before- $\alpha$ -interferon treatment data using the t test.

‡P values describe the comparison of after-imatinib treatment data with after- $\alpha$ -interferon treatment data using the t test.

**Table 3. Correlation analysis for paired cohort of imatinib-treated patients**

| Paired comparisons                  | Correlation coefficient* | P      |
|-------------------------------------|--------------------------|--------|
| TBV and serum phosphate             | -0.48                    | .004   |
| TBV and total calcium               | -0.42                    | .014   |
| TBV and ionized calcium             | -0.33                    | .059   |
| Serum phosphate and total calcium   | 0.47                     | .006   |
| Serum phosphate and ionized calcium | 0.48                     | .004   |
| Total calcium and ionized calcium   | 0.88                     | < .001 |

\*Spearman rank order correlation.

(Figure 5B). To investigate whether imatinib has a sustained effect on p38, Akt, and Crk-L activation, cell lysates were harvested from osteogenic cultures, treated with and without 3  $\mu$ M imatinib, at days 1, 7, and 14 of culture (Figure 5C). Levels of activated p38 remained consistent with basal levels at the time intervals examined, with no apparent inhibition by imatinib. Conversely, an increase above basal levels of activation was observed for Crk-L after days 7 and 14 of culture. Similarly, phosphorylated Akt was observed after days 7 and 14 of culture. Image quantitation revealed a 50% reduction in Akt activation in the presence of imatinib at days 7 and 14 and a 50% reduction in Crk-L activation on day 14 (data not shown).

Given the significant inhibition of PDGF-induced Akt activation by imatinib, we investigated whether inhibition of Akt could account for the increase in mineralized matrix seen in imatinib-treated cultures. To address this, we tested the effect of a PDGF-R inhibitor (AG-1295) and a PI3-kinase inhibitor (LY294002) on PDGF-induced Akt activation and osteoblast function. Initially, bone explant cultures were stimulated with PDGF in the presence of increasing concentrations of each drug to identify an inhibitory concentration. PDGF-induced Akt activation was significantly reduced at 25  $\mu$ M AG-1295 and 5  $\mu$ M LY294002, whereas Crk-L activation remained unaffected (Figure 6A). Bone explant cultures were then cultured under osteogenic conditions in the presence of the inhibitory concentration of each drug, and the amount of mineralized matrix was quantified. Cells cultured in the presence of

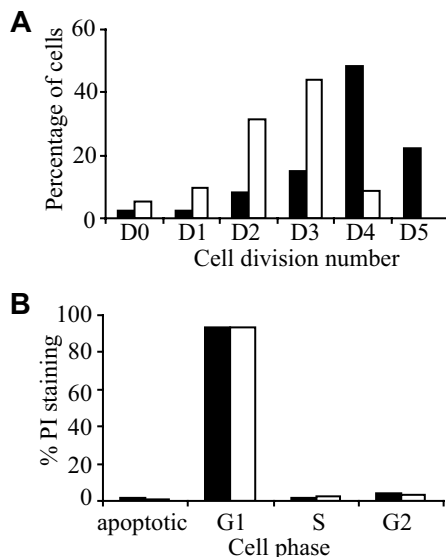


**Figure 2. Imatinib inhibits osteoblast proliferation but does not induce apoptosis.** Osteoblast cultures were stained with the fluorescent dye CFSE, cultured for a period of 7 days in the presence (□) or absence (■) of imatinib (3  $\mu$ M), then analyzed by flow cytometry. (A) Imatinib reduced the number of cell divisions compared with the untreated control. (B) To determine whether imatinib induced apoptosis, the effect of imatinib on cell cycling was examined using propidium iodide (PI). No difference in cell cycling was observed between untreated and imatinib treated cultures, with most cells accumulating in G<sub>1</sub> phase of the cell cycle.

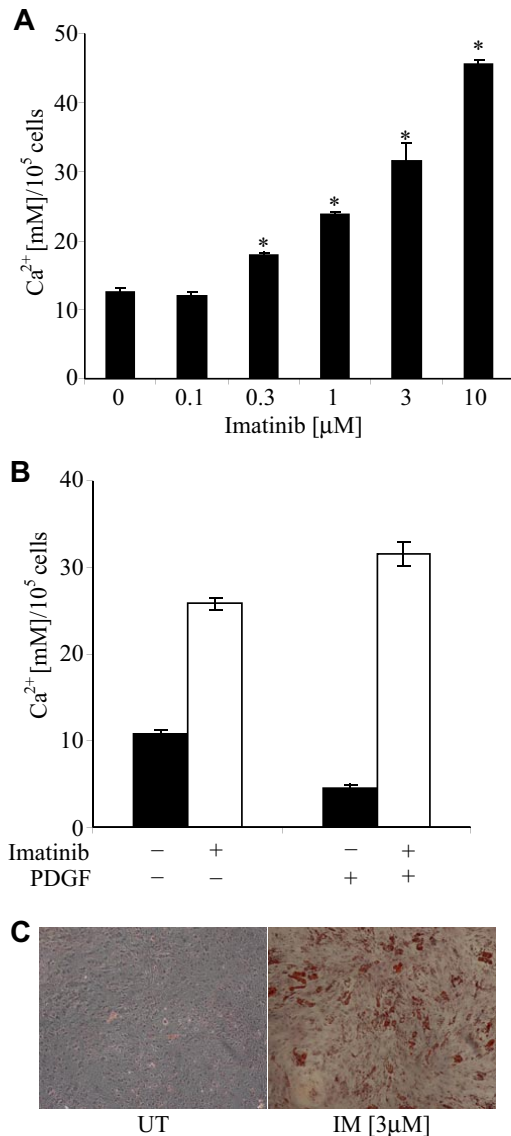


**Figure 3. Imatinib promotes mineral formation in bone trephine explant cultures.** (A) Posterior superior iliac spine bone trephine explant cultures were grown under osteoinductive conditions in the presence of various concentrations of imatinib for 4 weeks. Mineralized matrix was solubilized in 0.6 M HCl and the concentration of calcium per 10<sup>5</sup> cells quantified as previously described.<sup>20</sup> A dose-dependent increase in mineral formation was observed in the presence of imatinib. Mean values are shown; error bars represent the standard error of triplicate measurements. \**P* ≤ .05. (B) To examine whether the mechanism by which imatinib increased mineral formation was through inhibition of the PDGF receptor, mineralization assays were performed in the presence of exogenous PDGF-BB (10 ng/mL). The addition of PDGF-BB to control cultures (■) decreased mineral formation, which was overcome by the addition of 3  $\mu$ M imatinib (□). Mean values are shown; error bars represent the standard error of triplicate measurements. (C) In addition to promoting mineral formation, imatinib induced adipocyte formation in osteogenic cultures. Lipid droplets are stained with Oil Red O and cells counterstained with hematoxylin. Original magnification 40 $\times$ . UT denotes untreated cells; IM, imatinib-treated cells. Images acquired as detailed in the Figure 1 legend.

25  $\mu$ M AG-1295 and 5  $\mu$ M LY294002 produced more matrix (2.5-fold and 4-fold, respectively; Figure 6B) than untreated controls.

## Discussion

Changes in levels of bone-remodeling markers in patient sera have been observed in CML and GIST patients receiving imatinib

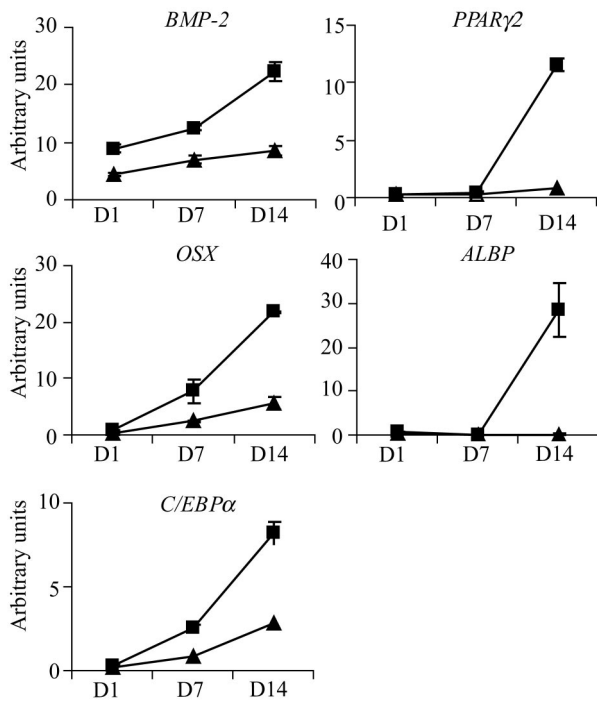


**Figure 4. Imatinib modulates the expression of genes involved in both osteogenic and adipogenic differentiation.** Bone trephine explant cultures grown under osteoinductive conditions were treated with (■) or without (▲) 3  $\mu$ M imatinib, and RNA was harvested on days 0, 1, 7, and 14. Quantitative real-time PCR was used to examine mRNA levels of key genes involved in osteoblast and adipocyte development. Treatment of cultures with imatinib up-regulated expression of osteoblast specific transcription factor osterix (*OSX*) and bone morphogenic protein 2 (*BMP-2*). Imatinib also up-regulated expression of adipocyte-specific transcription factors *C/EBP $\alpha$*  and *PPAR $\gamma$ 2* and the adipocyte-specific lipid transporter *ALBP*. For quantitative real-time analysis, expression levels were normalized to values obtained for  $\beta$ -actin. Mean values are shown; error bars represent the standard error of triplicate measurements.

therapy.<sup>15,16</sup> In this current study, we investigated whether these changes are reflected in bone biopsies taken from CML patients before and after imatinib therapy, and whether osteoblast proliferation and function were modulated by imatinib in vitro.

Histomorphometric analysis of bone was performed on routine (2-mm diameter) trephine biopsies that were decalcified and prepared for histologic examination. Although trephine diameter is not a variable that has been shown to affect histomorphometric quantitation,<sup>29</sup> decalcification limited our ability to distinguish between unmineralized (osteoid) and mineralized bone matrix, parameters important for the measurement of osteoblast function. Despite these limitations, we were able to measure the TBV, a key parameter of bone metabolism. Our analysis of bone biopsies (paired imatinib group, n = 17) revealed an increase in TBV in 76% (13 of 17) of patients, with 47% (8 of 17) of patients having at least a 2-fold increase in TBV. This increase was so substantial that the TBV in the second biopsy often exceeded the normal upper limit for the patient's age group. Importantly, an increase in TBV was detected in older adults (older than 50 years) and those with osteoporosis at diagnosis. Although it is conceivable that the differences in TBV may be attributable to differences in the site from which the preimatinib and postimatinib biopsies were retrieved, this is unlikely, as several studies report limited site-dependent differences in TBV throughout the ilium.<sup>18,30-33</sup>

The increase in TBV observed in imatinib-treated patients appears to be de novo bone formation, as most CML patients had trabecular bone volumes within normal ranges at diagnosis. Changes in bone morphometry are extremely rare in chronic-phase CML patients,<sup>22,34</sup> with most patients having normal TBV and osteoclast numbers before treatment.<sup>23</sup> The increase in TBV is unlikely to be attributable to a return to normal bone marrow cellularity after eradication of leukemic cells, as most  $\alpha$ -interferon treated CML patients who experienced a significant decrease in tumor burden showed no substantive increase in TBV. We did,

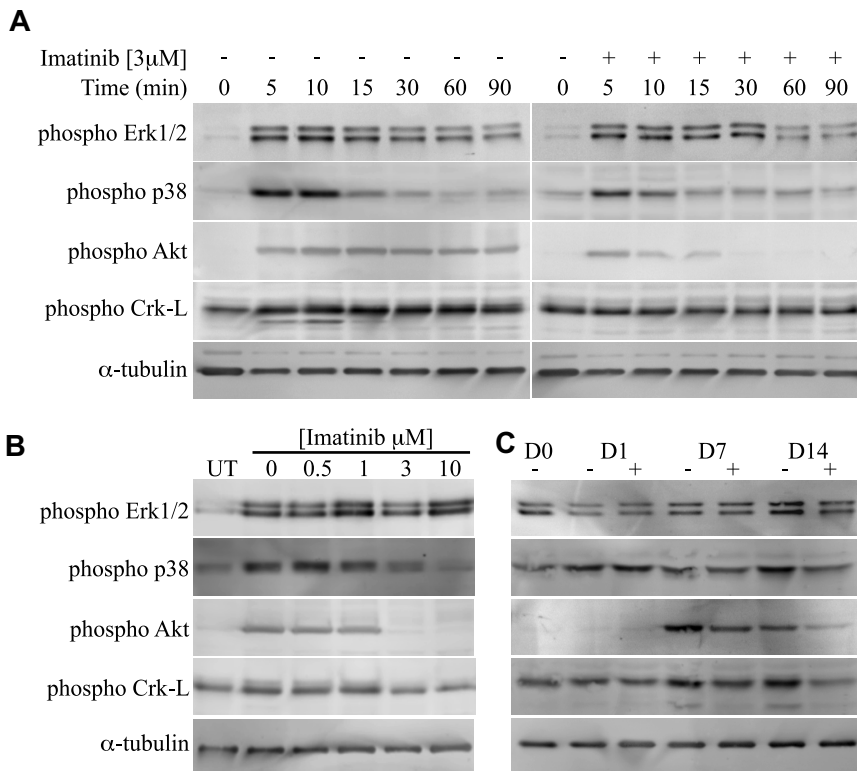


**Figure 5. Imatinib is a potent inhibitor of PDGF-induced Akt and Crk-L activation in osteoblast cells.** (A) Bone trephine explant cultures were serum deprived, treated with or without imatinib (3  $\mu$ M), then stimulated with PDGF-BB (10 ng/mL) for the indicated times, after which cell lysates harvested. Equivalent levels of cellular proteins were transferred to PVDF membranes and probed with phosphorylation-specific antibodies as indicated. (B) To determine the concentration range at which imatinib was inhibitory to PDGF-induced p38, Akt, and Crk-L phosphorylation, serum-deprived cells were treated with a range of imatinib concentrations, stimulated with PDGF (10 ng/mL) for 10 minutes, and then processed as above. Western blots were probed with phosphorylation-specific antibodies as indicated. Untreated lysates are labeled UT. (C) To determine whether imatinib had a sustained effect on p38, Akt, and Crk-L activation, lysates were harvested from osteogenic cultures treated with or without 3  $\mu$ M imatinib at weekly intervals for 2 weeks. Proteins were transferred to PVDF membranes and probed with phosphorylation-specific antibodies as indicated.

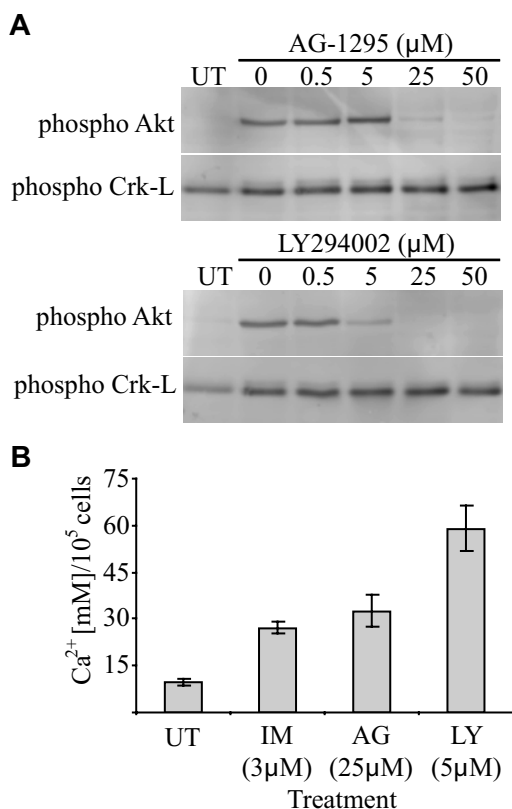


**Figure 6. Inhibition of Akt activation in osteoblasts promotes mineralized-matrix production.** (A) To determine the concentration range at which AG-1295 and LY294002 were inhibitory to PDGF-induced Akt phosphorylation, serum-deprived cells were treated with a range of drug concentrations and stimulated with PDGF (10 ng/mL) for 10 minutes, after which cell lysates harvested. Equivalent levels of cellular proteins were transferred to PVDF membranes and probed with phosphorylation-specific antibodies as indicated. (B) To determine the effect of the drugs on mineral formation, iliac crest bone trephine explant cultures were grown under osteoinductive conditions in the presence of an inhibitory concentration of the indicated drug for 4 weeks and the concentration of calcium per  $10^5$  cells was then quantified. IM represents imatinib; AG, AG-1295; LY, LY294002; and UT, untreated. Mean values are shown; error bars represent the standard error of triplicate measurements.

however, observe a 2-fold increase in TBV in 3  $\alpha$ -interferon treated patients, 2 of whom achieved clinical remission (Table S1). Consistent with our findings,  $\alpha$ -interferon has been shown to impose variable effects on the skeleton, albeit in other disease settings. Although some studies show that  $\alpha$ -interferon has no effect on bone mineral density (BMD),<sup>35,36</sup> other studies have shown an increase<sup>37</sup> or a decrease in BMD.<sup>38</sup>

The mechanism by which imatinib stimulates the increase in TBV remains speculative, as the hypercellularity of pretreatment bone biopsies prevented reliable determination of osteoclast and/or osteoblast numbers. Previously, we demonstrated that imatinib reduces osteoclast number and lacunae formation in adult BALB/c mice,<sup>3,5</sup> suggesting a similar inhibitory effect could occur in humans. Indeed, a reduction in serum N-telopeptide of collagen crosslinks, a marker of osteoclast activity, has been reported in CML and GIST patients after imatinib treatment.<sup>15</sup> Although the effect of imatinib treatment on osteoblast numbers in vivo awaits further investigation, our in vitro data suggest that imatinib suppresses mesenchymal cell proliferation. The observed increase in TBV may therefore be due to suppression of osteoclast differentiation and activity and/or an increase in osteoblast differentiation and activity. In support of this hypothesis, our in vitro functional data are consistent with imatinib promoting osteoblast differentiation and function by inhibiting PDGF signaling. PDGF is a potent osteoblast

mitogen and inhibitor of osteoblast differentiation.<sup>9-11</sup> Inhibition of PDGF by imatinib increased mineralized-matrix production and led to an increase in *OSX* and *BMP-2* expression, factors important for differentiation of preosteoblasts into functionally mature osteoblasts.<sup>39,40</sup> Other studies have suggested that localized administration or systemic administration of PDGF promotes bone formation in vivo.<sup>12,13</sup> However, as PDGF is a potent mesenchymal cell mitogen, it is difficult to determine whether the increase in bone is associated with a direct effect on osteoblast differentiation or with an indirect mitogenic effect. In contrast, suppression of PDGF signaling has been suggested to promote bone formation in an immunodeficient mouse bone engraftment model.<sup>41</sup>

In response to stimulation with PDGF, imatinib is a potent inhibitor of Akt, an important PI3-kinase substrate. In osteogenic cultures, imatinib had a sustained inhibitory effect on Akt activation, suggesting that inhibition of PDGF-induced PI3-kinase/Akt activation is important for osteoblast differentiation. PI3 kinase is a positive regulator of osteoblast survival<sup>42,43</sup> and differentiation<sup>44-46</sup> in response to factors such as BMP-2 and Wnt-3a. In response to PDGF, PI3 kinase is essential for PDGF-induced chemotaxis,<sup>46,47</sup> and recently PI3 kinase was shown to play an inhibitory role in osteoblast differentiation.<sup>41</sup> Inhibition of PDGF-induced PI3 kinase activation using wortmannin, a specific PI3-kinase inhibitor, promoted osteogenic differentiation and mineralized-matrix production.<sup>41</sup> In support of these findings, treatment of bone explant cultures with either a PI3-kinase inhibitor, LY294002, or a PDGF-R inhibitor, AG-1295, promoted mineralized-matrix production at concentrations that inhibited PDGF-induced activation of Akt. These findings are consistent with imatinib inhibiting PDGF-induced activation of PI3 kinase and Akt, thereby promoting mineralized-matrix production.

Imatinib also inhibited PDGF-induced activation of c-Abl, as measured by activation of Crk-L. In murine cells, c-Abl appears to play a positive role in osteogenic differentiation as osteoblasts isolated from c-Abl<sup>-/-</sup> mice have a reduced capacity to form mineralized matrix and to respond to osteogenic factors such as BMP-2.<sup>14</sup> c-Abl is also involved in actin reorganization in response to PDGF stimulation,<sup>48</sup> suggesting a role in cell migration and chemotaxis.<sup>49</sup> A role for c-Abl in the imatinib-mediated increase in mineral formation requires further investigation, as both LY294002 and AG-1295 promoted mineral formation without inhibiting Crk-L activation.

The ability of imatinib to regulate genes involved in both osteogenic and adipogenic differentiation is a reflection of the multilineage potential, and the degree of lineage commitment, of cells cultured from bone trephine explants.<sup>20,50</sup> Addition of imatinib to this mixed population of cells appears to promote differentiation of lineage-committed cells, resulting in the appearance of adipocytes in osteogenic cultures. PDGF is the primary mitogen and chemoattractant of mesenchymal cells and is thought to act as a negative regulator of adipogenesis.<sup>51,52</sup> The mechanism of this inhibitory action may involve activation of protein kinase C<sup>53</sup> or other signaling pathways, including the MAPK pathways.<sup>54</sup> Although suppression of Erk1/2 signaling in bone explant cultures promotes adipogenesis,<sup>21</sup> imatinib failed to modulate Erk1/2 activation in cultures stimulated with PDGF at 10 ng/mL or 1 ng/mL (data not shown). Conversely, imatinib suppressed activation of p38, which has been demonstrated to negatively regulate murine adipogenesis.<sup>55</sup> Further investigation is required to provide mechanistic insight into the effect of imatinib on mesenchymal cell differentiation.

As previously reported, CML and GIST patients treated with imatinib experience changes in markers of bone metabolism in their serum.<sup>15,16</sup> These changes are associated with a decrease in serum calcium and phosphate, secondary hyperparathyroidism, and



phosphaturia. Consistent with these findings, we observed a significant decrease in serum phosphate and calcium concentrations after imatinib therapy but not after  $\alpha$ -interferon treatment. It has been suggested that imatinib treatment results in a decrease in serum calcium, causing a compensatory increase in parathyroid hormone, which in turn decreases renal phosphate absorption, leading to hypophosphatemia.<sup>16</sup> Although there is agreement that imatinib does not appear to affect intestinal absorption of calcium, the mechanism leading to low serum calcium remains speculative. We have shown strong negative correlations between TBV and both serum phosphate and total calcium levels, suggesting a causative association. In light of our findings and those of previous studies,<sup>15,16</sup> we propose a model to explain the action of imatinib on bone remodeling (Figure 7). Imatinib restrains bone resorption (by inhibiting c-Fms on osteoclasts) and stimulates bone formation (by inhibiting PDGF-R on osteoblasts), resulting in sequestration of calcium and phosphate to bone. The decrease in serum calcium stimulates parathyroid hormone secretion, which decreases renal phosphate absorption, leading to hypophosphatemia.

In summary, we demonstrate for the first time that imatinib mesylate significantly modulates bone turnover, as evidenced by an increase in TBV and lowered levels of serum calcium and phosphate. Although we are unable to predict the long-term skeletal consequences of this drug, our study does suggest that patient management and care should include appropriate monitoring of skeletal health. Furthermore, the observed increase in TBV, a significant determinant of bone strength,<sup>56</sup> raises the intriguing possibility that imatinib and similar agents may have uses in treating diseases that are characterized by generalized bone loss, such as osteoporosis and osteomalacia. This possibility is particularly attractive in light of the long-term safety data that have accrued during imatinib's widespread use as a front-line therapy for CML and GIST. Based on these findings, our current efforts are focused on a broad-prospective study to investigate the effect of imatinib on the rate of bone formation, including bone densitometry and indices of bone turnover (resorption surface and total osteoid surface) using undecalcified bone biopsies, to determine the long-term implication of imatinib therapy on skeletal remodeling.

## Acknowledgments

Imatinib mesylate was kindly provided by Novartis Pharmaceuticals. We would also like to acknowledge Dr Peter Smith and Dr Ian Parkinson (Bone and Joint Laboratory, IMVS) for their assistance with the EDAX analysis.

This work was supported by grants from the National Health and Medical Research Council of Australia (A.L.D., L.B.T., T.P.H., and A.C.W.Z.).

## Authorship

Contribution: S.F. and A.L.D. designed and performed research, analyzed data, and wrote the manuscript; P.K. performed research and analyzed data; L.B.T., T.P.H., and M.M.R. collected data, provided intellectual input, and provided critical feedback on the manuscript; K.L. contributed reagents (imatinib [Gleevec]) and

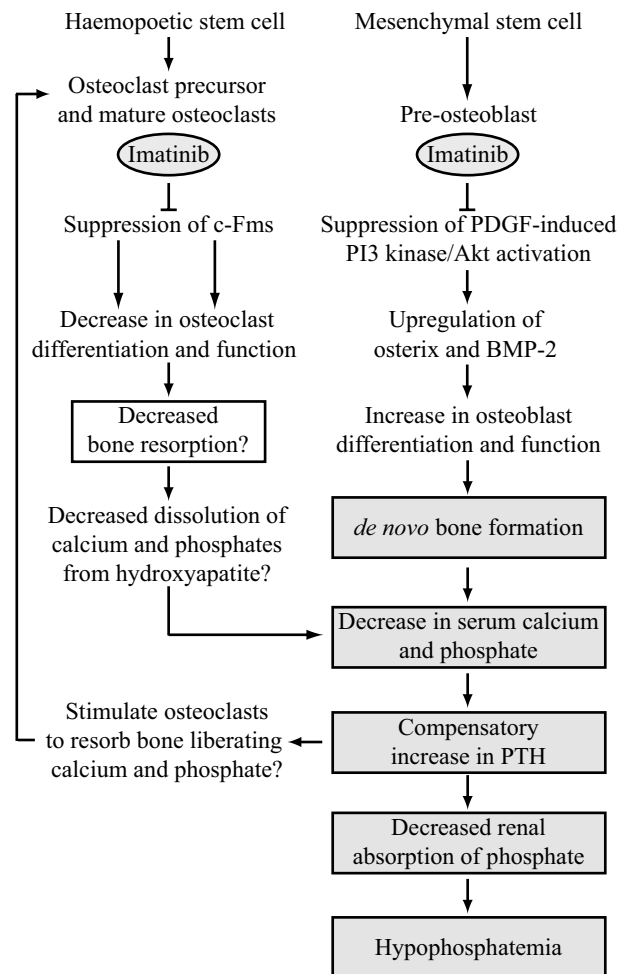


**Figure 7. Proposed model of the effect of imatinib mesylate on bone remodeling.** Imatinib suppresses osteoclast differentiation and function through inhibition of c-Fms, resulting in a decrease in dissolution of calcium and phosphate from bone. Concomitantly, imatinib promotes osteoblast function through inhibition of PDGF-R, resulting in *de novo* bone formation. Sequestration of calcium and phosphate to bone results in a net decrease in extracellular calcium and phosphate, which in turn stimulates a compensatory increase in parathyroid hormone (PTH) release. PTH liberates calcium and phosphate from bone by stimulating osteoclast activity. This process is potentially suppressed by imatinib. PTH also balances extracellular calcium and phosphate levels, resulting in a decrease in renal phosphate absorption. This decrease further depletes serum phosphate levels, leading to hypophosphatemia. Shaded boxes represent processes that have been confirmed *in vivo* and include observations made in previous studies.<sup>15,16</sup>

provided critical feedback on the manuscript; B.V.-R. performed all histomorphometry, analyzed data, and provided critical feedback on the manuscript; and A.C.W.Z. provided intellectual input, designed research, assisted with data analysis, and provided critical feedback on the manuscript.

Conflict-of-interest disclosure: K.L. is a full-time employee of Novartis Pharmaceuticals. The other authors declare no competing financial interests.

Correspondence: Andrew Zannettino, Myeloma and Mesenchymal Research Group, Bone and Cancer Research Laboratories, Division of Haematology, Institute of Medical and Veterinary Science, Hanson Institute, GPO Box 14, Adelaide, South Australia, 5000; e-mail: andrew.zannettino@imvs.sa.gov.au.

## References

- Demetri GD, von Mehren M, Blanke CD, et al. Efficacy and safety of imatinib mesylate in advanced gastrointestinal stromal tumors. *N Engl J Med*. 2002;347:472-480.
- Apperley JF, Gardembas M, Melo JV, et al. Response to imatinib mesylate in patients with

- chronic myeloproliferative diseases with rearrangements of the platelet-derived growth factor receptor beta. *N Engl J Med*. 2002;347:481-487.
3. Dewar AL, Cambarelli AC, Zannettino AC, et al. Macrophage colony-stimulating factor receptor c-fms is a novel target of imatinib. *Blood*. 2005;105:3127-3132.
  4. Tanaka S, Takahashi N, Udagawa N, et al. Macrophage colony-stimulating factor is indispensable for both proliferation and differentiation of osteoclast progenitors. *J Clin Invest*. 1993;91:257-263.
  5. Dewar AL, Farrugia AN, Conchina MR, et al. Imatinib as a potential antiresorptive therapy for bone disease. *Blood*. 2006;107:4334-4337.
  6. Grigoriadis AE, Heersche JN, Aubin JE. Differentiation of muscle, fat, cartilage, and bone from progenitor cells present in a bone-derived clonal cell population: effect of dexamethasone. *J Cell Biol*. 1988;106:2139-2151.
  7. Grigoriadis AE, Heersche JN, Aubin JE. Continuously growing bipotential and monopotent myogenic, adipogenic, and chondrogenic subclones isolated from the multipotential RCJ 3.1 clonal cell line. *Dev Biol*. 1990;142:313-318.
  8. Yamaguchi A, Kahn AJ. Clonal osteogenic cell lines express myogenic and adipocytic developmental potential. *Calcif Tissue Int*. 1991;49:221-225.
  9. Hock JM, Canalis E. Platelet-derived growth factor enhances bone cell replication, but not differentiated function of osteoblasts. *Endocrinology*. 1994;134:1423-1428.
  10. Kubota K, Sakikawa C, Katsumata M, Nakamura T, Wakabayashi K. Platelet-derived growth factor BB secreted from osteoclasts acts as an osteoblastogenesis inhibitory factor. *J Bone Miner Res*. 2002;17:257-265.
  11. Chaudhary LR, Hofmeister AM, Hruska KA. Differential growth factor control of bone formation through osteoprogenitor differentiation. *Bone*. 2004;34:402-411.
  12. Nash TJ, Howlett CR, Martin C, Steele J, Johnson KA, Hicklin DJ. Effect of platelet-derived growth factor on tibial osteotomies in rabbits. *Bone*. 1994;15:203-208.
  13. Millak BH, Finkelman RD, Hill EL, et al. The effect of systemically administered PDGF-BB on the rodent skeleton. *J Bone Miner Res*. 1996;11:238-247.
  14. Li B, Boast S, de los Santos K, et al. Mice deficient in Abl are osteoporotic and have defects in osteoblast maturation. *Nat Genet*. 2000;24:304-308.
  15. Berman E, Nicolaidis M, Maki RG, et al. Altered bone and mineral metabolism in patients receiving imatinib mesylate. *N Engl J Med*. 2006;354:2006-2013.
  16. Grey A, O'Sullivan S, Reid IR, Browett P. Imatinib mesylate, increased bone formation, and secondary hyperparathyroidism. *N Engl J Med*. 2006;355:2494-2495.
  17. Revell PA. Quantitative methods in bone biopsy examination. In: Revell PA, ed. *Pathology of Bone*. Berlin: Springer-Verlag; 1986:87-111.
  18. Melsen F, Melsen B, Mosekilde L, Bergmann S. Histomorphometric analysis of normal bone from the iliac crest. *Acta Pathol Microbiol Scand [A]*. 1978;86:70-81.
  19. Gundle R, Stewart K, Screen J, Beresford JN. Isolation and culture of human bone-derived cells. In: Beresford JN, Owen ME, eds. *Marrow Stromal Cell Culture*. Cambridge: Cambridge University Press; 1998:43-66.
  20. Gronthos S, Zannettino AC, Graves SE, Ohta S, Hay SJ, Simmons PJ. Differential cell surface expression of the STRO-1 and alkaline phosphatase antigens on discrete developmental stages in primary cultures of human bone cells. *J Bone Miner Res*. 1999;14:47-56.
  21. Jaiswal RK, Jaiswal N, Bruder SP, Mbalaviele G, Marshak DR, Pittenger MF. Adult human mesenchymal stem cell differentiation to the osteogenic or adipogenic lineage is regulated by mitogen-activated protein kinase. *J Biol Chem*. 2000;275:9645-9652.
  22. Frydecka I, Bieniek J, Brodzka W. Osteolytic lesion in chronic myelogenous leukaemia. *Folia Haematol Int Mag Klin Morphol Blutforsch*. 1984;111:610-613.
  23. Thiele J, Hoepfner B, Wienhold S, Schneider G, Fischer R, Zankovich R. Osteoclasts and bone remodeling in chronic myeloproliferative disorders. A histochemical and morphometric study on trephine biopsies in 165 patients. *Pathol Res Pract*. 1989;184:591-599.
  24. Baccarani M, Saglio G, Goldman J, et al. Evolving concepts in the management of chronic myeloid leukemia: recommendations from an expert panel on behalf of the European LeukemiaNet. *Blood*. 2006;108:1809-1820.
  25. le Coutre P, Kreuzer KA, Pursche S, et al. Pharmacokinetics and cellular uptake of imatinib and its main metabolite CGP74588. *Cancer Chemother Pharmacol*. 2004;53:313-323.
  26. Lyons AB, Parish CR. Determination of lymphocyte division by flow cytometry. *J Immunol Methods*. 1994;171:131-137.
  27. Jaiswal N, Haynesworth SE, Caplan AI, Bruder SP. Osteogenic differentiation of purified, culture-expanded human mesenchymal stem cells in vitro. *J Cell Biochem*. 1997;64:295-312.
  28. Sattler M, Salgia R, Okuda K, et al. The proto-oncogene product p120CBL and the adaptor proteins CRKL and c-CRKL link c-ABL, p190BCR/ABL and p210BCR/ABL to the phosphatidylinositol-3' kinase pathway. *Oncogene*. 1996;12:839-846.
  29. Moore RJ, Durbridge TC, Woods AE, Vernon-Roberts B. Comparison of two bone trephine instruments used for quantitative histomorphometry. *J Clin Pathol*. 1989;42:213-215.
  30. Garner A, Ball J. Quantitative observations on mineralised and unmineralised bone in chronic renal azotaemia and intestinal malabsorption syndrome. *J Pathol Bacteriol*. 1966;91:545-561.
  31. Beck JS, Nordin BE. Histological assessment of osteoporosis by iliac crest biopsy. *J Pathol Bacteriol*. 1960;80:391-397.
  32. Melsen F, Melsen B, Mosekilde L. An evaluation of the quantitative parameters applied in bone histology. *Acta Pathol Microbiol Scand [A]*. 1978;86:63-69.
  33. Moore RJ, Durbridge TC, Woods AE, Vernon-Roberts B. Variation in histomorphometric estimates across different sites of the iliac crest. *J Clin Pathol*. 1989;42:814-816.
  34. Nadal E, Cervantes F, Rosinol L, Talam C, Montserrat E. Hypercalcemia as the presenting feature of t-cell lymphoid blast crisis of ph-positive chronic myeloid leukemia. *Leuk Lymphoma*. 2001;41:203-206.
  35. Solis-Herruzo JA, Castellano G, Fernandez I, Munoz R, Hawkins F. Decreased bone mineral density after therapy with alpha interferon in combination with ribavirin for chronic hepatitis C. *J Hepatol*. 2000;33:812-817.
  36. Kauppila M, Koskinen P, Pulkki K, et al. Interferon-alpha treatment decreases serum cross-linked C-terminal telopeptide of type I collagen in haematological diseases. *Clin Lab Haematol*. 2000;22:15-20.
  37. Avnet S, Cenni E, Perut F, et al. Interferon-alpha inhibits in vitro osteoclast differentiation and renal cell carcinoma-induced angiogenesis. *Int J Oncol*. 2007;30:469-476.
  38. Pérez Castrillón JL, Cano-del Pozo M, Sanz-Izquierdo S, Velayos-Jiménez J, Dib-Wobakin W. Bone mineral density in patients with multiple sclerosis: the effects of interferon [in Spanish]. *Rev Neurol*. 2003;36:901-903.
  39. Yamaguchi A, Katagiri T, Ikeda T, et al. Recombinant human bone morphogenetic protein-2 stimulates osteoblastic maturation and inhibits myogenic differentiation in vitro. *J Cell Biol*. 1991;113:681-687.
  40. Nakashima K, Zhou X, Kunkel G, et al. The novel zinc finger-containing transcription factor osterix is required for osteoblast differentiation and bone formation. *Cell*. 2002;108:17-29.
  41. Kratchmarova I, Blagoev B, Haack-Sorensen M, Kassem M, Mann M. Mechanism of divergent growth factor effects in mesenchymal stem cell differentiation. *Science*. 2005;308:1472-1477.
  42. Debais F, Lefèvre G, Lemonnier J, et al. Fibroblast growth factor-2 induces osteoblast survival through a phosphatidylinositol 3-kinase-dependent, -β-catenin-independent signaling pathway. *Exp Cell Res*. 2004;297:235-246.
  43. Almeida M, Han L, Bellido T, Manolagas SC, Kousteni S. Wnt proteins prevent apoptosis of both uncommitted osteoblast progenitors and differentiated osteoblasts by beta-catenin-dependent and -independent signaling cascades involving Src/ERK and phosphatidylinositol 3-kinase/AKT. *J Biol Chem*. 2005;280:41342-41351.
  44. Ghosh-Choudhury N, Abboud SL, Nishimura R, Celeste A, Mahimainathan L, Choudhury GG. Requirement of BMP-2-induced phosphatidylinositol 3-kinase and Akt serine/threonine kinase in osteoblast differentiation and Smad-dependent BMP-2 gene transcription. *J Biol Chem*. 2002;277:33361-33368.
  45. Vinals F, Lopez-Rovira T, Rosa JL, Ventura F. Inhibition of PI3K/p70 S6K and p38 MAPK cascades increases osteoblastic differentiation induced by BMP-2. *FEBS Lett*. 2002;510:99-104.
  46. Fujita T, Azuma Y, Fukuyama R, et al. Runx2 induces osteoblast and chondrocyte differentiation and enhances their migration by coupling with PI3K-Akt signaling. *J Cell Biol*. 2004;166:85-95.
  47. Fukuyama R, Fujita T, Azuma Y, et al. Statins inhibit osteoblast migration by inhibiting Rac-Akt signaling. *Biochem Biophys Res Commun*. 2004;315:636-642.
  48. Plattner R, Kadlec L, DeMai KA, Kazlauskas A, Pendergast AM. c-Abl is activated by growth factors and Src family kinases and has a role in the cellular response to PDGF. *Genes Dev*. 1999;13:2400-2411.
  49. Plattner R, Koleske AJ, Kazlauskas A, Pendergast AM. Bidirectional signaling links the Ablon kinases to the platelet-derived growth factor receptor. *Mol Cell Biol*. 2004;24:2573-2583.
  50. Pittenger MF, Mackay AM, Beck SC, et al. Multipotential potential of adult human mesenchymal stem cells. *Science*. 1999;284:143-147.
  51. Summers SA, Whiteman EL, Cho H, Lipfert L, Birnbaum MJ. Differentiation-dependent suppression of platelet-derived growth factor signaling in cultured adipocytes. *J Biol Chem*. 1999;274:23858-23867.
  52. Koellensperger E, von Heimburg D, Markowicz M, Pallua N. Human serum from platelet-poor plasma for the culture of primary human preadipocytes. *Stem Cells*. 2006;24:1218-1225.
  53. Artemenko Y, Gagnon A, Aubin D, Sorisky A. Anti-adipogenic effect of PDGF is reversed by PKC inhibition. *J Cell Physiol*. 2005;204:646-653.
  54. Bost F, Aouadi M, Caron L, Binetruy B. The role of MAPKs in adipocyte differentiation and obesity. *Biochimie*. 2005;87:51-56.
  55. Aouadi M, Laurent K, Prot M, Le Marchand-Brustel Y, Binetruy B, Bost F. Inhibition of p38MAPK increases adipogenesis from embryonic to adult stages. *Diabetes*. 2006;55:281-289.
  56. Felsenberg D, Boonen S. The bone quality framework: determinants of bone strength and their interrelationships, and implications for osteoporosis management. *Clin Ther*. 2005;27:1-11.